Parallel kinetic Monte Carlo simulations of two-dimensional island coarsening

Feng Shi,* Yunsic Shim,† and Jacques G. Amar‡
Department of Physics and Astronomy, University of Toledo, Toledo, Ohio 43606, USA
(Received 2 June 2007; published 28 September 2007)

The results of parallel kinetic Monte Carlo (KMC) simulations of island coarsening based on a bond-counting model are presented. Our simulations were carried out both as a test of and as an application of the recently developed semirigorous synchronous sublattice (SL) algorithm. By carrying out simulations over long times and for large system sizes the asymptotic coarsening behavior and scaled island-size distribution (ISD) were determined. Our results indicate that while cluster diffusion and coalescence play a role at early and intermediate times, at late times the coarsening proceeds via Ostwald ripening. In addition, we find that the asymptotic scaled ISD is significantly narrower and more sharply peaked than the mean-field theory prediction. The dependence of the scaled ISD on coverage is also studied. Our results demonstrate that parallel KMC simulations can be used to effectively extend the time scale over which realistic coarsening simulations can be carried out. In particular, for simulations of the late stages of coarsening with system size $L=1600$ and eight processors, a parallel efficiency larger than 80% was obtained. These results suggest that the SL algorithm is likely to be useful in the future in parallel KMC simulations of more complicated models of coarsening.

DOI: 10.1103/PhysRevE.76.031607 PACS number(s): 68.43.Jk, 68.35.Fx, 02.70.−c

I. INTRODUCTION

Coarsening plays an important role in a wide variety of processes ranging from grain growth in alloys [1], to soot formation [2], to the formation of galaxies [3]. One example of particular current interest is the coarsening of two-dimensional (2D) or three-dimensional islands on a surface [4], since the coarsening process determines the nanoscale ordering and surface structure. As a result, island coarsening has recently been the subject of a large amount of experimental and theoretical work [4–14].

For the case of 2D clusters on a surface, it is useful to consider two particular limiting regimes in which the coarsening is dominated by diffusion—Ostwald ripening [15,16] and cluster diffusion and coalescence [5–13]. In the case of Ostwald ripening the islands are assumed to be immobile, while the coarsening is mediated by a background density of diffusing atoms such that islands bigger than a critical island size grow while smaller islands shrink or evaporate. This results in power-law growth of the average island size $S(t)$ corresponding to the average number of atoms in an island, i.e., $S(t)\sim t^{2n}$ where $n=1/3$ for the case of 2D clusters on a 2D substrate [17,18]. It also leads to a scale invariant island-size distribution at late time. In the case of cluster diffusion and coalescence, power-law growth of the average island size and a scale-invariant island-size distribution are also observed. In particular, if the cluster diffusion coefficient $D(s)$ decays as a power law with island size s, i.e., $D(s)\sim s^{-x}$, then $n=1/2(1+x)$ [5]. Three different limiting cases have been considered to be of particular interest [6–12]—cluster diffusion due to periphery diffusion ($x=3/2$, $n=1/5$), cluster diffusion due to correlated evaporation and/or condensation ($x=1$, $n=1/4$), and finally cluster diffusion due to uncorrelated evaporation and/or condensation ($x=1/2$, $n=1/3$). Although asymptotically, one might expect one of these processes to dominate for a particular case, in general one might expect all these processes to play a role.

Besides the coarsening exponent, one quantity of particular interest is the asymptotic scaled island-size distribution. In particular, if $N_s(t)$ is the density of islands of size s at time t (where s is the number of atoms in an island) then one may write [19]

$$f(s/S)=S^2N_s(t)/\theta, \tag{1}$$

where $S(t)=\Sigma sN_s/\Sigma N_s$ is the average island size and θ is the coverage and $f(u)$ is the scaled island-size distribution (ISD). At late time one expects that $f(u)$ will be independent of time. We note that there have been a number of theoretical efforts to determine the asymptotic scaled ISD and its dependence on coverage. For example, for the case of Ostwald ripening the mean-field theory of Lifshitz-Slyozov-Wagner (LSW) leads to an analytical expression for the scaled ISD which is valid in the limit $\theta\rightarrow 0$. However, for finite coverage one expects that correlations may play a significant role. As a result, there have also been a number of theoretical attempts [20–24] to extend the LSW theory to finite coverage in two and three dimensions, although these efforts have focused primarily on the low-coverage limit in which islands may be treated as isolated droplets. For the case of 2D island coarsening, a number of numerical simulations have also recently been carried out [25–28]. However, because of the role of correlations as well as the relatively slow convergence to the asymptotic distribution, determining the asymptotic scaled ISD remains a challenging problem.

Here we present the results of parallel kinetic Monte Carlo (KMC) simulations of 2D island coarsening which were carried out using our recently developed synchronous sublattice (SL) algorithm [29]. We note that in contrast to a variety of other algorithms for parallel KMC via domain decomposition which are rigorous and which require global

*fengshi@physics.utoledo.edu
†yshim@physics.utoledo.edu
‡jamar@physics.utoledo.edu

communications [30–33], the SL algorithm only requires local communications with nearest-neighbor processors. As a result it is both relatively simple to implement and in general significantly more efficient. In particular, for a fixed processor size, we have demonstrated [29] that it exhibits linear scaling as a function of the number of processors, i.e., the parallel speed-up is proportional to the number of processors. On the other hand, it is only semirigorous [29]. Therefore, it is of interest to examine the accuracy and efficiency of the SL algorithm in simulations of coarsening, since we have so far only applied it to parallel KMC simulations of growth. In addition we would like to use it to compare the asymptotic island-size distribution with the predictions of theories of Ostwald ripening. As discussed in more detail below, we find that the SL algorithm can indeed be used to accurately and efficiently carry out parallel KMC simulations of island coarsening, and in contrast to previous work on a similar model [25], we are able to reach the asymptotic scaling regime corresponding to $n=1/3$. Our results also indicate that the asymptotic scaled island-size distribution is significantly different from the prediction of a recent mean-field theory of Ostwald ripening at finite coverage developed by Yao *et al.* [24]. We believe that this is due to the existence of correlations as well as cluster diffusion which are not taken into account in Ref. [24].

The organization of this paper is as follows. In Sec. II, we describe the bond-counting model used in our coarsening simulations and then briefly review the SL algorithm. In Sec. III, we present a comparison between parallel and serial results for the average island size and island-size distribution at early and intermediate times in order to validate our long time simulation results. We then present our parallel KMC results for the evolution of the average island size and island-size distribution at much longer times along with a comparison with the theory of Yao *et al.* [24] for two different coverages, $\theta=0.1$ and $\theta=0.2$. We also study the efficiency of the SL algorithm and its dependence on the number of processors and cycle time. Finally, in Sec. IV, we discuss our results.

II. MODEL AND SIMULATIONS

Since one of the main goals of this work is to carry out a first test of the accuracy and efficiency of the SL algorithm when applied to coarsening, we have considered the simplest possible model, corresponding to "bond counting" on a square lattice. In particular, in our model atoms are assumed to diffuse in all four possible nearest-neighbor directions with a configuration-dependent hopping rate D_n given by

$$D_n = \nu_0 e^{-E_a/k_B T}, \tag{2}$$

where the prefactor $\nu_0=10^{12}$ s^{-1}, $E_a=E_0+nE_b$ is the configuration-dependent activation energy, E_0 corresponds to the activation energy for monomer diffusion, $n=0-4$ is the number of in-plane nearest neighbors, and T is the substrate temperature. In our simulations a value $E_0=0.4$ eV, which is a typical value for metal (100) surfaces, was assumed along with a moderate "bond strength" $E_b=0.1$ eV, while our coarsening simulations were carried out at a temperature $T=250$ K. We note that Lam *et al.* [25] have recently carried out KMC simulations of island coarsening at 700 K using a similar bond-counting model, but using larger values for the activation energies for diffusion ($E_0=1.3$ eV and $E_b=0.3$ eV) which are more typical of semiconductors. However, once the higher coarsening temperature is taken into account, the effective parameters (E_0/k_BT and E_b/k_BT) are close to those used in the model previously studied by Lam *et al.* [25].

In order to study the asymptotic coarsening behavior, as well as the coverage dependence, we have carried out simulations of coarsening at two different coverages, $\theta=0.1$ and $\theta=0.2$. In each case, the initial island distribution was prepared by depositing particles with deposition rate $F=1$ ML/s at $T=250$ K up to the desired coverage. Starting at this point ($t=0$) coarsening simulations were then carried out over times ranging from 10^3 s to 10^5 s while periodic boundary conditions were assumed. For the very short time simulations, system sizes of $L=256$ and $L=512$ were used, while for the much longer time simulations, systems of size $L=1600$ were used to avoid finite-size effects. In order to obtain good statistics, the short time results were typically averaged over 500 runs while the longer time results were averaged over 78 runs. In all of our simulations the island-size distribution N_s (where N_s is the density of islands of size s) was measured along with the total island density $N=\Sigma_{s\geq 2}N_s$, monomer density N_1, and average island size $S=\frac{1}{N}\Sigma_{s\geq 2}sN_s=(\theta-N_1)/N$.

While serial KMC simulations were used for comparison and for testing, in order to reach longer times, most of our simulations were carried out using the recently developed semirigorous synchronous sublattice parallel KMC algorithm [29] with strip geometry. In this algorithm, different parts of the system are assigned via spatial decomposition to different processors. However, in order to avoid conflicts between processors due to the synchronous nature of the algorithm, each processor's domain is further divided into different regions or sublattices. In particular, for the case of strip geometry considered here, our square system was divided into N_p strips (where N_p is the number of processors) of width $N_x=L/N_p$ with each strip corresponding to a different processor. Each strip was then divided into two halves—one corresponding to a A sublattice and the other corresponding to a B sublattice. A complete synchronous cycle corresponding to a time interval τ is then as follows. At the beginning of a cycle, each processor's local time is initialized to zero. One of the sublattices is then randomly selected so that all processors operate on the same sublattice during that cycle. Each processor then simultaneously and independently carries out KMC events in the selected sublattice until the time when the next event exceeds the time interval τ. As in the usual serial KMC, each event is carried out with time increment $\Delta t_i=-\ln(r_i)/R_i$, where r_i is a uniform random number between 0 and 1, and R_i is the total event rate for that sublattice. Each processor then communicates any necessary changes (boundary events) with its neighboring processors, updates its event rates, and moves on to the next cycle using a new randomly chosen sublattice.

We note that in the standard SL algorithm the cycle time τ must be smaller than the inverse of the fastest possible

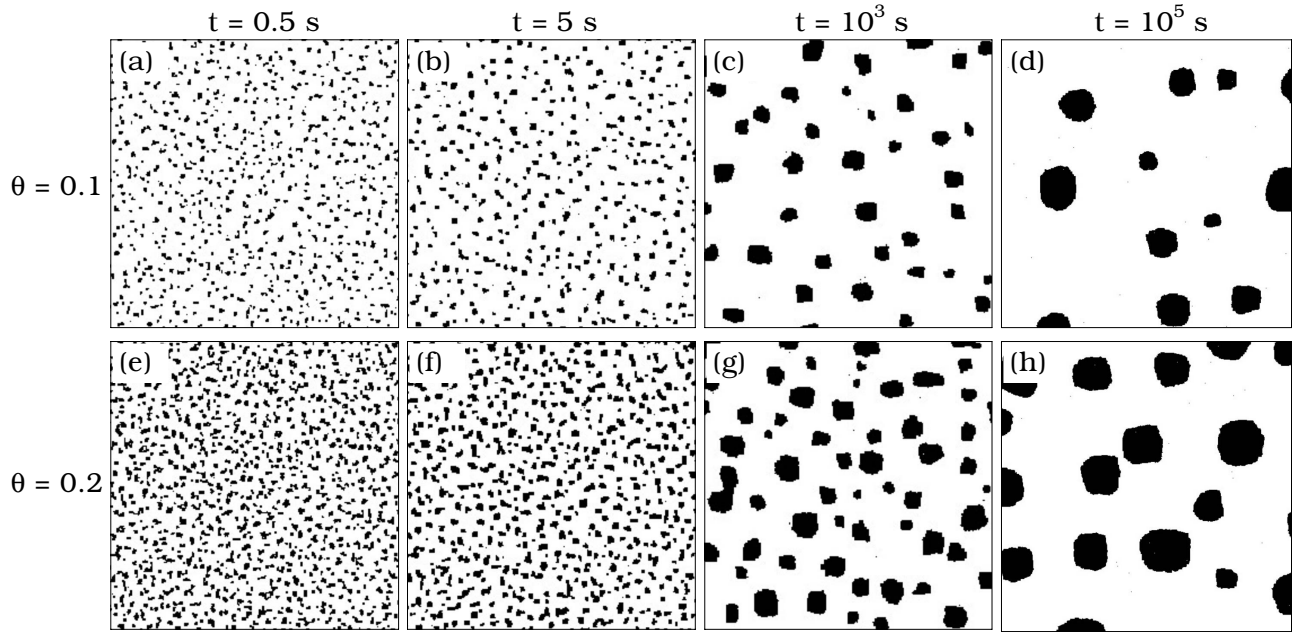

FIG. 1. System morphology at different times for $\theta=0.1$ and $\theta=0.2$. Pictures correspond to 256×256 portions of a 1024×1024 system.

single-event rate in the system [29]. This ensures that, for example, particles near the processor or sublattice boundary will only move once (on average) before moving on to the next cycle and so will not be "trapped" in the "ghost" region just outside the boundary. Accordingly, in most of our parallel simulations a value $\tau=1/D_0$ was used for the cycle time. In our previous tests of this algorithm using a variety of models of epitaxial growth [29] it was found that using such an upper bound on the cycle time led to results which were identical to serial KMC results—except for extremely small processor sizes ($N_x\leq8$) when the sublattice size was less than a "diffusion length." However, we have also carried out additional test simulations of coarsening with a larger cycle time since this may increase the parallel efficiency. As our results demonstrate, in the case of coarsening, the cycle time can be significantly increased without affecting the accuracy.

In order to study the asymptotic coarsening behavior while avoiding finite-size effects, our long time parallel KMC simulations ($t=10^5$ s) were carried out using large system sizes ($L=1600$) with $N_p=8$. However, in order to validate our parallel KMC results we have first carried out short and intermediate time tests ($t=10^2-10^3$ s) in which we have compared serial and parallel simulation results for different numbers of processors N_p. In these tests systems of size $L=256$ and 512 were used, while the number of processors ranged from $N_p=1$ (serial) to $N_p=64$. We note that the processor width N_x ranged from L (serial runs) to very small values ($N_x=4$) for the case of $L=256$ with $N_p=64$.

III. RESULTS

Figure 1 shows typical results for the system morphology as a function of time up to $t=10^5$ s for $\theta=0.1$ and $\theta=0.2$, for the case $L=1024$. As can be seen, while the islands are initially very small and somewhat irregular, with increasing time the average island-size increases while the islands become smoother and appear to approach a "squarelike" shape with rounded corners. We now present results for the comparison between serial and parallel simulations before studying in more detail the quantitative evolution of the average island-size and island-size distribution.

A. Comparison of serial and parallel results

As a first test of the accuracy of our parallel KMC simulations, we have compared serial results for the monomer and island densities as a function of time up to $t=10^3$ s at coverage $\theta=0.1$ (system size $L=256$) with the corresponding parallel results obtained with the SL algorithm with cycle time $\tau=1/D_0$ and the number of processors ranging from $N_p=4$ ($N_x=64$) to $N_p=64$ ($N_x=4$). As can be seen in Fig. 2(a), both the island and monomer densities decrease with time although the island density appears to be decreasing more quickly. The small value of the monomer density also indicates that to a good approximation the average island size S is directly related to the island density N, i.e., $S\simeq\theta/N$. In addition, we find that for all values of N_p there is excellent agreement between the parallel and serial results for the island density even for extremely small processor sizes, thus indicating that there is a negligible finite processor-size effect. Similar agreement is obtained for the monomer density N_1 (see Fig. 2) although for the very smallest processor size ($N_x=4$, $N_p=64$) there is a small finite processor size for the monomer density, i.e., the monomer density obtained in the parallel simulations is slightly higher than the serial result. Figure 2(b) shows similar results for the scaled ISD at $t=100$ s for a slightly larger system size ($L=512$) with the number of processors ranging from $N_p=1$ (serial) to $N_p=64$. As can be seen, there is essentially no

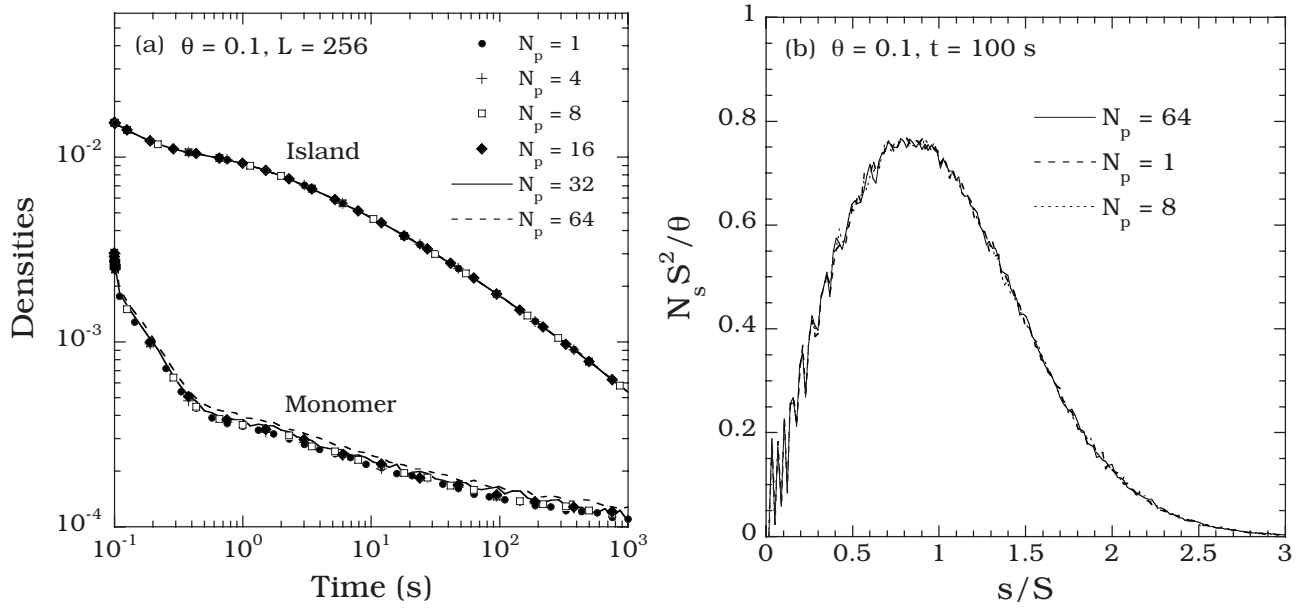

FIG. 2. Comparison of serial and parallel coarsening results at short and intermediate times for different values of N_p ($N_x=L/N_p$) at $\theta=0.1$. All results are averaged over 500 runs. (a) Monomer and island densities ($L=256$). (b) Scaled ISD at $t=100$ s for system size $L=512$.

difference between the serial and parallel KMC results for the scaled ISD. These results indicate that, somewhat surprisingly, the finite processor-size effect in island coarsening is significantly weaker than during submonolayer island growth [29]. We attribute this to the fact that the process of coarsening is somewhat closer to equilibrium than nucleation and island growth.

B. Asymptotic coarsening behavior and scaled island-size distribution

Based on these results, we have carried out parallel KMC simulations over much longer times ($t=10^5$ s) and much larger system sizes ($L=1600$) with $N_p=8$ ($N_x=200$) in order to determine the asymptotic behavior. We note that the processor width ($N_x=200$) in these simulations is significantly larger than the largest processor width ($N_x=4$) for which a noticeable finite-processor size effect was observed. In order to obtain good statistics our results were averaged over 78 runs. Figure 3 shows the corresponding simulation results for the average island size S as a function of time for $\theta=0.1$ and $\theta=0.2$. As can be seen, after an initial "transient" period, there is an "intermediate" period from $t=10-10^3$ s during which an effective slope of 1/2 corresponding to a coarsening exponent $n\simeq 1/4$ is obtained. We note that this value corresponds to the correlated evaporation-condensation mechanism for cluster diffusion [7] and is also consistent with the observation of significant cluster diffusion and coalescence during this period. However, at later times ($t>10^3$ s) the slope approaches the asymptotic value of 2/3 corresponding to a coarsening exponent $n=1/3$. While such an exponent is consistent with both cluster diffusion due to uncorrelated evaporation-condensation and Ostwald ripening, we have observed that there is significantly less cluster diffusion and coalescence during this late time period. Instead, what is observed is that the smaller clusters evaporate while the larger clusters grow, as in Ostwald ripening. Such a scenario is also consistent with the fact that, as indicated by the inset in Fig. 3, at late time the island density is smaller than the monomer density. Thus, at late time the islands are essentially in quasiequilibrium with a "gas" of monomers as is assumed in Ostwald ripening. We now consider the time evolution of the scaled ISD as well as the dependence of the asymptotic ISD on coverage.

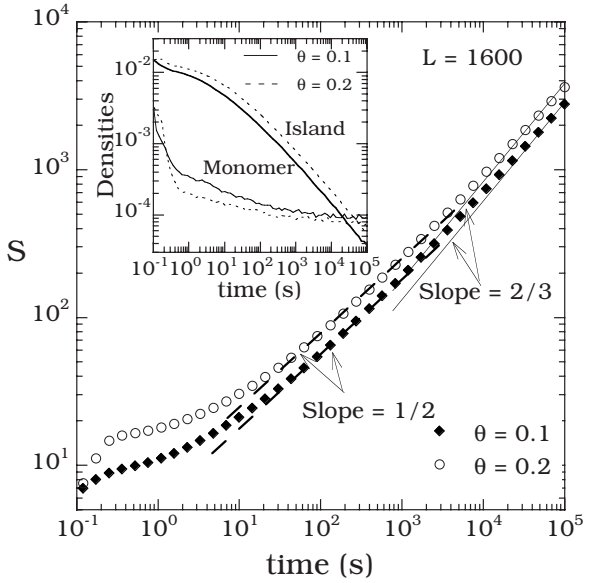

FIG. 3. Average island size S as a function of time for coverages $\theta=0.1$ and $\theta=0.2$ (system size $L=1600$). Inset shows corresponding results for island and monomer densities.

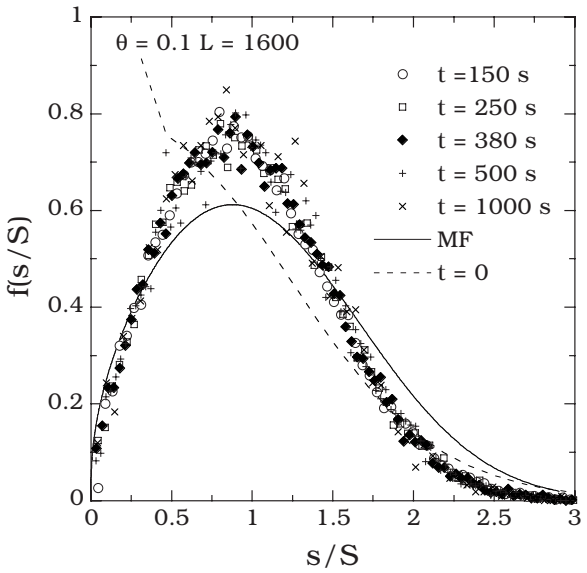

FIG. 4. Comparison between parallel KMC simulation results for scaled ISD at early and intermediate time (θ=0.1) and mean-field (MF) prediction of Yao *et al.* [24].

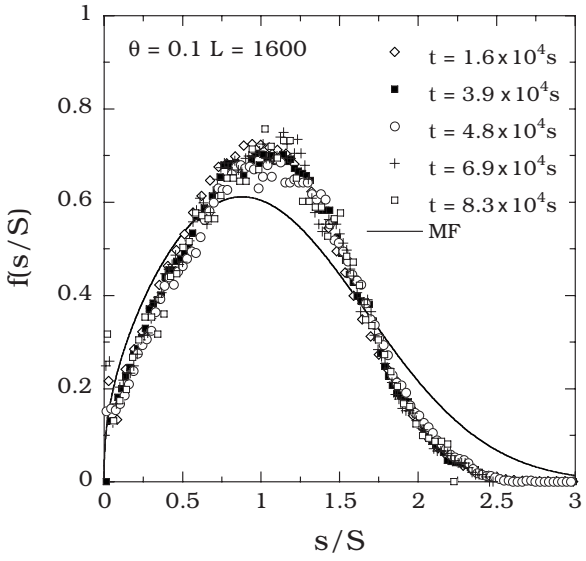

FIG. 5. Comparison between parallel KMC simulation results for scaled ISD at late time (θ=0.1) and mean-field prediction of Yao *et al.* [24].

Figure 4 shows our results for the scaled island-size distribution,

$$f(s/S) = N_s(t)S^2/\theta, \tag{3}$$

at early and intermediate times (t=150−10^3 s) along with the initial scaled ISD at t=0 (dashed curve). We note that these simulations were carried out using L=1600 with N_p=16. Also shown is the prediction of the mean-field theory of Yao *et al.* [24] (solid curve) for 2D Ostwald ripening and θ=0.1, which was obtained by numerically solving the system of self-consistent equations given in Ref. [24]. We note that in 2D the theory of Yao *et al.* [24] is based on the assumption of circular islands, and leads to a prediction for the "scaled droplet distribution function" $g(r/R)$ where r is the cluster radius, R is the average island radius, and $S=\pi R^2$. In order to convert this result to a scaled ISD we have used the relation $f(u)=g(\sqrt{u})/(2\sqrt{u})$. As can be seen in Fig. 4 our simulation results exhibit good scaling over a relatively large range of times, thus indicating that the scaled ISD is approaching its asymptotic behavior. However, there are significant deviations between the simulation results and the asymptotic mean-field theory prediction of Yao *et al.* [24]. In particular, the scaled ISD obtained from our KMC simulations is narrower and higher than the Yao model prediction.

Figure 5 shows our parallel KMC results for the scaled ISD at much longer times (approximately 100 times longer) for system size L=1600 and N_p=8. As can be seen, at late times the peak of the scaled ISD is slightly lower and is also slightly shifted to the right compared to the ISD at intermediate times but is still significantly different from the mean-field (MF) prediction of Yao *et al.* In particular, the peak of the distribution is still significantly higher and narrower than the Yao *et al.* [24] prediction while the peak position corresponds to a scaled island-size close to 1, in contrast to the prediction of Yao *et al.* In addition, both the small s/S portion of the distribution as well as the tail ($s/S>2.0$) deviate even more strongly from the MF prediction than at intermediate times. We believe that these deviations are due to the existence of correlations which are not taken into account in the MF theory.

In order to study the coverage dependence of the scaled ISD we have also carried out simulations of coarsening at coverage θ=0.2, as shown in Fig. 6. As can be seen, our simulation results for the scaled ISD at θ=0.2 are very similar to those obtained at θ=0.1, thus indicating a relatively weak coverage dependence. We note that for comparison, also shown in Fig. 6 (solid and dashed curves) are the predictions of Yao *et al.* [24] for the asymptotic scaled ISD for coverages θ=0.1 and θ=0.16. We note that while these re-

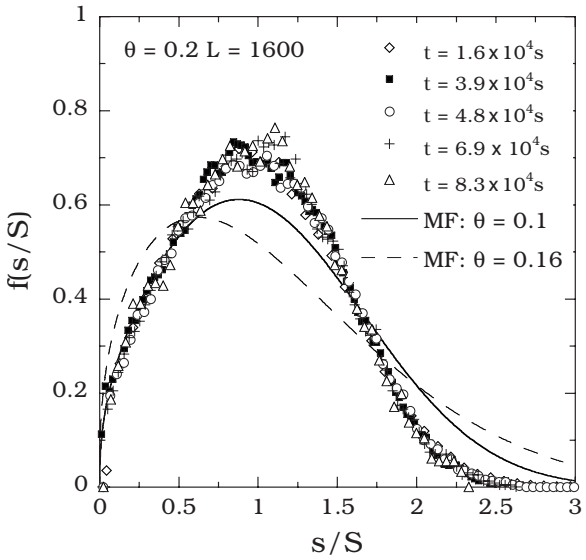

FIG. 6. Comparison of KMC simulation results for the scaled ISD at late time (θ=0.2) and the mean-field predictions of Yao *et al.* [24] at θ=0.1 (solid curve) and θ=0.16 (dashed curve).

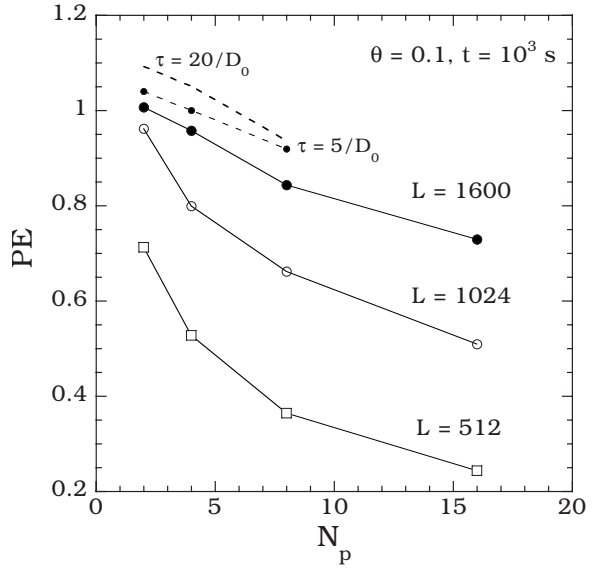

FIG. 7. Parallel efficiency (PE) as a function of number of processors N_p. Solid lines correspond to results obtained using $\tau = 1/D_0$, while dashed lines correspond to results for $L=1600$ using a larger value of τ (see text).

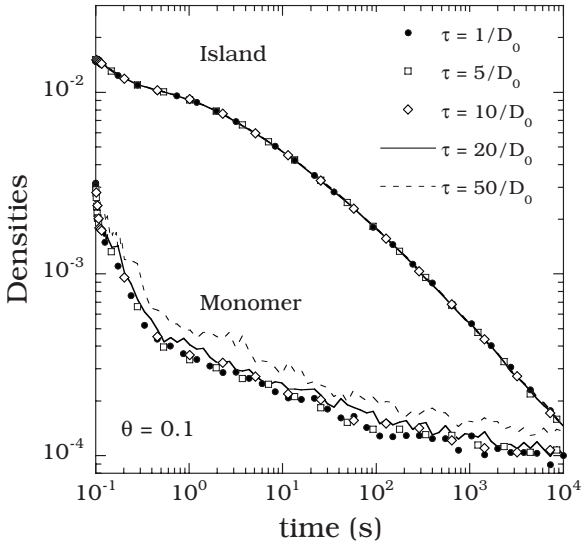

FIG. 8. Evolution of monomer and island densities obtained using SL algorithm with different values of cycle time τ ($L=1600$ and $N_p=8$).

sults were obtained by numerically solving the system of self-consistent equations given in Ref. [24], for values of θ larger than 0.16 it appears that there are numerical instabilities in the solution of the self-consistent equations used by Yao *et al.* [24]. As a result, this theory could not be used to obtain a prediction for $\theta=0.2$. In any case, a comparison between our scaled ISD results for $\theta=0.2$ with the MF predictions for $\theta=0.1$ and $\theta=0.16$ indicates that at larger coverage the discrepancy between the simulation results and the MF prediction increases. This may be due in part to the fact that this theory is only applicable at relatively small coverage such that the screening length (corresponding roughly to the distance between islands) is significantly larger than the island radius.

C. Dependence of parallel efficiency on N_p and cycle time τ

We now consider the parallel efficiency obtained in our parallel KMC simulations. We note that in our simulations, the parallel efficiency was calculated using the expression

$$\mathrm{PE} = \frac{t_{\mathrm{serial}}}{N_p \; t_{\mathrm{parallel}}}, \tag{4}$$

where t_{serial} corresponds to the time for a serial simulation and t_{parallel} corresponds to the time for a parallel simulation of the same system with N_p processors. The solid lines in Fig. 7 indicate our results for the parallel efficiency obtained from test runs of length $t=10^3$ s as a function of the number of processors N_p for different system sizes $L=512$, 1024, and 1600 using a cycle time $\tau=1/D_0$. As expected, for fixed system size L the parallel efficiency decays with increasing N_p due to the decrease in the processor size and number of events per cycle. This leads to an increase in the relative communications overhead as well as in the relative fluctuations in the number of events per processor which implies a decreased utilization per processor. However, for fixed N_p the parallel efficiency increases with increasing L since this leads to an increased processor size. We note that for the parameters used in most of our simulations ($L=1600$, $N_p=8$) the parallel efficiency is slightly larger than 80%.

We now consider the effects of increasing the cycle time τ on the accuracy and efficiency of our parallel KMC simulations. We note that in previous work on parallel KMC simulations of submonolayer and multilayer growth using the SL algorithm [29], we found that a "conservative" cycle time corresponding to the inverse of the fastest possible single-event rate was required to maintain the accuracy of the parallel simulation. Accordingly all of the coarsening results presented so far were obtained using such a "conservative" cycle time $\tau=1/D_0$. However, it is of interest to investigate the effect of increasing the cycle time τ since this may increase the parallel efficiency of the simulations by decreasing the relative fluctuation in the number of events in each processor as well as the communications overhead. In addition, we expect that since coarsening is a "slow" process which is close to equilibrium, there should be less dependence on the cycle time than in the previously studied cases of submonolayer and multilayer growth [29].

Figure 8 shows the island and monomer densities during coarsening ($\theta=0.1$) obtained in parallel simulations with $L=1600$ and $N_p=8$ for different values of the cycle time ranging from $\tau=1/D_0$ to $\tau=50/D_0$. As can be seen there is essentially no dependence of the island density on the cycle time for all values of τ, while the monomer density agrees within error bars for all values of τ up $10/D_0$. However, for longer cycle times ($\tau \geq 20/D_0$) there are noticeable deviations in the monomer density. This relatively weak dependence on the cycle time τ is in striking contrast to our previous results for simple nonequilibrium growth models and is due, we suspect to the fact that coarsening is much closer to equilibrium. The corresponding results for the parallel efficiency are shown in Fig. 7 (dashed lines). As can be seen,

using $\tau=5/D_0$ leads to a significant increase in the parallel efficiency for the case of $L=1600$ with $N_p=8$, while using a significantly longer cycle time ($\tau=20/D_0$) does not further improve the parallel efficiency. We also note that for $N_p=2$, using $\tau=5/D_0$ leads to a parallel efficiency which is slightly larger than 1. This is due to the existence of cache effects which have a stronger effect in serial simulations than in parallel simulations due to the larger processor size [32].

IV. DISCUSSION

We have presented the results of parallel kinetic Monte Carlo simulations of 2D island coarsening using our recently developed semirigorous synchronous SL algorithm. Our results indicate that parallel simulations can be used to effectively extend the time scale over which realistic coarsening simulations can be carried out. In particular, using a conservative cycle time $\tau=\tau_0=1/D_0$ corresponding to the inverse of the fastest possible single-event rate, we have demonstrated that the SL algorithm leads to results which are identical to those obtained using serial KMC except for extremely small processor sizes. In addition, for system sizes which were not too small the parallel efficiency was found to be relatively large. In particular, for our simulations of the late stages of coarsening with system size $L=1600$ and $N_p=8$, a parallel efficiency larger than 80% was obtained.

We have also used the SL algorithm to carry out parallel KMC simulations of the asymptotic coarsening behavior for our bond-counting model, which is similar to that previously studied by Lam *et al.* [25]. We note that, in part because of the longer simulation times available via our parallel simulations, our coarsening exponents are significantly larger than obtained previously by Lam *et al.* [25], and so we were able to observe the asymptotic coarsening behavior. In particular, an asymptotic growth exponent $n\simeq 1/3$ was obtained for both $\theta=0.1$ and $\theta=0.2$. In addition, our results indicate that while cluster diffusion and coalescence play a role at early and intermediate times up to about 10^3 s, at late times the coarsening proceeds via Ostwald ripening.

By carrying out simulations of coarsening over long times and for large system sizes we have also studied the asymptotic behavior of the scaled ISD. For both $\theta=0.1$ and $\theta=0.2$, we find that the asymptotic scaled ISD is reached fairly quickly, i.e., there are only small changes in the scaled ISD for $t>10^3$ s. However, the scaled ISD's obtained in our simulations are significantly narrower and more sharply peaked than the mean-field theory predictions. As already noted, we believe that these deviations are primarily due to the existence of correlations which are not taken into account in the MF theory. However, other factors such as the existence of significant cluster diffusion for small islands in our model (due to evaporation condensation), as well as the shape of our islands (which are square rather than circular) might also play a role.

Finally, we have also compared the results of parallel KMC simulations of coarsening carried out using cycle times larger than the maximum "conservative" cycle time τ_0 with the corresponding serial results. Somewhat surprisingly, we found that for cycle times as large as $10\tau_0$ our results for the island and monomer densities are identical to the serial results. Interestingly, for even larger cycle times the island density is still unaffected, although there are noticeable deviations in the monomer density. This is in contrast to our previous studies of submonolayer and multilayer nucleation and growth using the SL algorithm [29,34], in which a cycle time significantly longer than the inverse of the fastest possible single-event rate led to results for the island density which deviate from the serial results. We believe that this relative insensitivity to the cycle time is due to the fact that coarsening is closer to equilibrium than nucleation and growth.

In conclusion, we have used the recently developed SL algorithm to carry out parallel kinetic Monte Carlo simulations of a simple bond-counting model of 2D island coarsening. Our results for this model indicate that while cluster diffusion via correlated evaporation-condensation and coalescence play a role at early and intermediate times, at late times the coarsening proceeds via Ostwald ripening. In addition, we found that the asymptotic scaled ISD is significantly narrower and more sharply peaked than the mean-field theory prediction of Yao *et al.* [24]. Our results also indicate that the SL algorithm can be used to effectively extend the time scale over which realistic coarsening simulations can be carried out. Based on these results we expect that the SL algorithm will be useful in the future in parallel KMC simulations of more complicated models of coarsening.

ACKNOWLEDGMENTS

This work was supported by the NSF through Grants Nos. CCF-0428826 and DMR-0606307. The authors would also like to acknowledge grants of computer time from the Ohio Supercomputer Center (Grant No. PJS0245).

[1] C. V. Thompson, Solid State Phys. **55**, 269 (2001).
[2] R. Dhaubhadel, F. Pierce, A. Chakrabarti, and C. M. Sorensen, Phys. Rev. E **73**, 011404 (2006).
[3] L. Searle and R. Zinn, Astrophys. J. **225**, 357 (1978).
[4] M. Zinke-Allmang, L. C. Feldman, and M. H. Grabow, Surf. Sci. Rep. **16**, 377 (1992).
[5] P. Meakin, Physica A **165**, 1 (1990).
[6] J. M. Wen, S.-L. Chang, J. W. Burnett, J. W. Evans, and P. A. Thiel, Phys. Rev. Lett. **73**, 2591 (1994).
[7] Clinton DeW. Van Siclen, Phys. Rev. Lett. **75**, 1574 (1995).
[8] S. V. Khare, N. C. Bartelt, and T. L. Einstein, Phys. Rev. Lett. **75**, 2148 (1995).
[9] D. S. Sholl and R. T. Skodje, Phys. Rev. Lett. **75**, 3158 (1995).
[10] D. S. Sholl and R. T. Skodje, Physica A **231**, 631 (1996).
[11] J. M. Soler, Phys. Rev. B **53**, R10540 (1996).
[12] W. W. Pai, A. K. Swan, Z. Zhang, and J. F. Wendelken, Phys.

Rev. Lett. **79**, 3210 (1997).
[13] D. Kandel, Phys. Rev. Lett. **79**, 4238 (1997).
[14] G. R. Carlow and M. Zinke-Allmang, Phys. Rev. Lett. **78**, 4601 (1997).
[15] W. Ostwald, Z. Phys. Chem. **37**, 385 (1901).
[16] P. W. Voorhees, J. Stat. Phys. **38**, 231 (1985).
[17] I. M. Lifshitz and V. V. Slyozov, J. Phys. Chem. Solids **19**, 35 (1961).
[18] C. Wagner, Z. Elektrochem. **65**, 581 (1961).
[19] M. C. Bartelt and J. W. Evans, Phys. Rev. B **46**, 12675 (1992).
[20] J. A. Marqusee and J. Ross, J. Chem. Phys. **80**, 536 (1984).
[21] M. Tokuyama and K. Kawasaki, Physica A **123**, 386 (1984).
[22] M. Marder, Phys. Rev. Lett. **55**, 2953 (1985); Phys. Rev. A **36**, 858 (1987).
[23] Q. Zheng and J. D. Gunton, Phys. Rev. A **39**, 4848 (1989).
[24] J. H. Yao, K. R. Elder, H. Guo, and M. Grant, Phys. Rev. B **47**, 14110 (1993).
[25] P.-M. Lam, D. Bayayoko, and X.-Y. Hu, Surf. Sci. **429**, 161 (1999).
[26] T. R. Mattsson, G. Mills, and H. Metiu, J. Chem. Phys. **110**, 12151 (1999).
[27] A. Lo and R. T. Skodje, J. Chem. Phys. **112**, 1966 (2000).
[28] M. Petersen, A. Zangwill, and C. Ratsch, Surf. Sci. **536**, 55 (2003).
[29] Y. Shim and J. G. Amar, Phys. Rev. B **71**, 125432 (2005).
[30] S. G. Eick, A. G. Greenberg, B. D. Lubachevsky, and A. Weiss, ACM Trans. Model. Comput. Simul. **3**, 287 (1993).
[31] B. D. Lubachevsky and A. Weiss, *Proceedings of the 15th Workshop on Parallel and Distributed Simulation* (IEEE, Piscataway, NJ, 2001); see also http://lanl.arXiv.org/abs/cs.DC/0405053.
[32] Y. Shim and J. G. Amar, Phys. Rev. B **71**, 115436 (2005).
[33] M. Merrick and K. A. Fichthorn, Phys. Rev. E **75**, 011606 (2007).
[34] Y. Shim and J. G. Amar, Phys. Rev. B **73**, 035423 (2006).